On the Relation Between Synthesis Parameters and Morphology of Anionic Polycaproamide Obtained in Organic Media. I. Influence of the $Na[O(CH_2)_2OCH_3]_2AlH_2$/ Isophorone Diisocyanate Catalytic System

CLEOPATRA VASILIU-OPREA* and FLORIN DAN

Department of Macromolecules, "Gh. Asachi" Technical University, 6600 Jassy, Romania

SYNOPSIS

Polycaproamide granules were obtained by anionic polymerization of caprolactam in ethylbenzene, using the sodium *bis*(2-methoxyethoxy)aluminium hydride/isophorone diisocyanate catalytic system. Under these conditions, polymerization occurs heterogeneously and the nature of the particle growth seems to be essentially a microbulk one. The most suitable reaction conditions were established. The morphology of the granules was investigated by scanning electron microscopy. These granules result from the coalescence of a great number of small, spherical particles. The coalescence occurs during solidification of the separated polymer. Numerous globular formations were observed at the surface of the particles. The particles were individualized through mechanical dispersion and measured, and the average number of particles composing the aggregates was calculated. Using wide-angle X-ray scattering and differential scanning calorimetry technics, the crystalline structure of the granular polycaproamide was studied. It contains almost entirely the α phase. The heat of fusion decreases slightly as compared with that corresponding to the anionic bulk polycaproamide. A schematic mechanism containing the stages involved in the obtaining of the granular polycaproamide is proposed. © 1996 John Wiley & Sons, Inc.

INTRODUCTION

Anionic polymerization of caprolactam (CL) in the presence of the sodium salt of caprolactam and carbon dioxide in xylene was first reported by Chrzczonowicz.[1,2] Later, different catalytic systems and solvents were used to obtain granular or powdered polycaproamide.[3-7] These forms are very convenient for many processing procedures, such as: flame spraying, electrostatic coating, pastes production, dispersions, and lacquer binders. Due to its extended surface, powdered polycaproamide may be also applied as an adsorbent. The polycaproamide obtained in hydrocarbon solvents exhibits high-molecular-weight homogeneity and relatively high average molecular weight.[8,9]

The chemical structure of the solvent-prepared polycaproamide is different from that corresponding to the anionic polycaproamide obtained in bulk. Bulk polymerization occurs at high temperatures, in a polar solvent (molten caprolactam which acts as a solvent of the polymer) and in a very strong basic media. Under these conditions, complex side reactions are favored. They include hydrogen abstraction from the C—H bonds situated in the α-position with respect to amide carbonyls, the acylation reaction of α-C anions of *N*-acylcaprolactam leading to various β-ketoimides and β-ketoamides, and subsequent Claisen-type condensation reactions of these compounds.[10-12] At high temperatures the amide groups may interchange and the local overheating can cause thermal degradation of the macromolecules and decarboxylation reactions. Condensations and disproportionations are also possible, favoring the appearance of new macromolecules both during the propagation stage and following the es-

* To whom correspondence should be addressed.

Journal of Applied Polymer Science, Vol. 62, 1517–1527 (1996)
 CCC 0021-8995/96/101517-11

tablishing of the monomer–polymer equilibrium. Furthermore, when approaching the end of the reaction, as the monomer is depleted, hydrogen abstraction can lead to branching.[13] As a result of the above-mentioned reactions and of some other side reactions, the polymers are branched or even crosslinked and are characterized by increased molecular inhomogeneity.

The anionic polymerization in solvents takes place mainly heterogeneously, in a mixture consisting of a "solvent" (CL) and a nonsolvent (the hydrocarbon). The liquid medium facilitates the transport of monomer and components of the catalytic system to the growing macromolecules. Thus, immediately after the initiation, i.e., in the first stages of the process, the macromolecules grow faster. They have greater chances to grow in the homogeneous liquid phase than the macromolecules beginning to grow later, when the concentration of CL decreases and the medium becomes a poorer solvent. This favors a more rapid precipitation of the chains, and when their number is significantly high the formation of aggregates may occur. These aggregates influence the diffusion phenomena and hinder the access of the CL anion to the growing macromolecules. The result is the premature stopping of the reactions; consequently, the conversion and the average molecular weight are diminished as compared with those corresponding to bulk polymerization polymers. The mild temperatures and the decreased basicity limit the side reactions leading to branched polymers. Thus the obtained macromolecules possess a regular structure and their molecular weight distribution is more homogeneous. The polymer contains a considerable fraction of macromolecules with high molecular weight and a small amount of macromolecules with lower molecular weight. The last ones are formed in the later stages of polymerization when the reaction medium contains monomer in low concentrations.[14]

The differences between the above-mentioned processes, bulk and solvent anionic polymerization of CL, may determine not only differences in molecular weight distribution and/or in the chemical structure of the macromolecules but also in the fine morphologic structure (porosity, density, crystalline forms, crystallinity). However, only few reports on the morphology of granular or powdered polycaproamide are available.

The present paper is concerned with the morphology of granular polycaproamide obtained by anionic polymerization of CL initiated with sodium *bis*(2-methoxyethoxy)aluminium hydride and activated with isophorone diisocyanate (IDI) in ethylbenzene (EB).

EXPERIMENTAL

Materials

RedAl 3.4*M* solution of sodium *bis*(2-methoxyethoxy)aluminium hydride in toluene and IDI (Aldrich) were used as received. CL (technical grade; Fibrex S.A. Savinesti, Romania) was twice recrystallized from benzene and dried in vacuum at 50°C. EB (technical grade; Carom S.A. Borzesti, Romania) was distilled with metallic sodium and benzophenone, stored over CaH_2 and redistilled at reduced pressure just before polymerization.

Synthesis of Granular Polycaproamide

The polymerization was carried out in a 150-mL glass flask fitted with thermometer, mechanical stirrer, reflux condenser, and inlet for dry nitrogen. The reaction flask was placed in a paraffin oil bath and the temperature in the thermostat was maintained within ±1°C. In a typical synthesis, CL (6 g) was dissolved in 18 mL EB at 80°C and subsequently RedAl (1.9 mL) was added. When the reaction was completed—as indicated by no hydrogen evolving—the temperature was quickly raised to 130°C and the activator (IDI, 0.25 mL) was added. After 20 min the polymerization was stopped by cooling, and the reaction mixture was transferred into methanol. The polymer was filtered, purified by extraction in a Soxhlet with methanol, and dried at 50°C and 50 Pa for 24 h.

Characterization

Average molecular weights were determined by viscometry using the following relation[15]:

$$[\eta] = 22.6 \cdot 10^{-3} \cdot M^{0.82}$$

Viscosity measurements were carried out in an Ubbelhode viscometer with capillary no. 1 (Schott & Gen Mainz) in 85% formic acid as solvent at 25 ± 0.05°C and at a concentration of 0.5 g/dL. Flow times were recorded as an average of three runs.

Scanning electron photomicrographs were obtained using a JEOL JSM 840 scanning electron microscope. The surface of the investigated samples was coated with platinum before examination.

Differential scanning calorimetry (DSC) analyses were performed with a General 4.0 D DuPont 2100 system, at heating and cooling rates of 10 and 5°C/min, respectively, under nitrogen atmosphere.

Wide-angle X-ray scattering measurements were made with a HZG-4A/2 diffractometer. The scattering curves were taken in the 8–32° interval using the step-scanning mode with the step of 0.1°.

RESULTS AND DISCUSSION

Polymerization

The anionic polymerization of CL proceeds by a two-step propagation mechanism. The propagating center is a cyclic amide linkage of the *N*-acylcaprolactam. To this, the monomer anion, "activated monomer," adds and rapidly opens the ring at the chain end and replaces it with another caprolactam molecule. The cycle is completed when the ^{-}N in the chain abstracts a hydrogen proton to form another active caprolactam anion.

The propagation is initiated through *N*-acyllactam species. These can be synthetized *in situ* or preformed and then added to the reaction system. The presence of the *exo*-carbonyl group attached to the nitrogen in *N*-acylcaprolactam increases the reactivity of the amide ring structure toward nucleophilic attack by the lactam anion.

Since the nucleophilic attack of lactam anion to the *N*-acyllactam group of activator is the rate-determining step,[16] the overall polymerization rate and furthermore the sequence of events occuring during the polymerization process can be controlled by a suitable choice of the catalytical system (activator and initiator). Thus, the polymerization rate increases with increasing the electrophilicity of the *exo*-cyclic carbonyl C-atom of *N*-acylcaprolactam[17–19] (this being related to the chemical structure of the residue, *R*, attached to it) and with increasing the nucleophilicity or dissociation degree of the lactam salt.[20]

In this report, the RedAl/IDI catalytic system was used. This system is suitable for the anionic polymerization of CL in solvents, i.e., it joins the lower nucleophilicity of initiator—"the reduced lactam salt"[21] (structure **A**) formed after monomer deprotonation—with the increased electrophilicity of *endo*-carbonyl group of *N*-(carbamoyl)caprolactam formed *in situ* through the reaction between CL and isocyanate. Also, the reduced hydride being soluble in the solvent, the local overheatings and consequently the side reactions are limited. In addition, by using diisocyanates against monoisocyanates, a

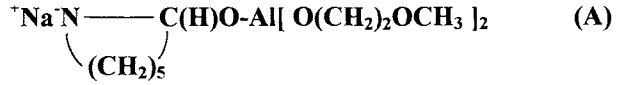

(A)

theoretical 2-fold average molecular weight could be obtained.

The polymerization begins in a homogeneous medium. The time period characterizing homogeneity is related to the synthesis parameters (e.g., at 130°C, about 60–140 s). Following this period, the reaction medium becomes translucent and after a very short period of time, below 4 s, this one becomes clear and white dispersed grains can be observed.

The influence of the most important reaction parameters (temperature, initial concentration of CL, amount of catalyst, and activator/catalyst ratio) on the conversion and degree of polymerization was investigated. As shown in Table I, both characteristics are strongly related to the synthesis parameters.

Both conversion and the degree of polymerization increase with the increase in the temperature. However, in the 80–120°C temperature range, the values of these characteristics increase significantly, while for temperatures higher than 120°C they present only slight increases.

In the presence of large amounts of solvent, the concentrations of both monomer and catalytic system decrease and consequently the overall polymerization rate decreases too. In addition, the reaction medium becomes a poorer solvent for the growing macromolecules, this favors a rapid precipitation and solidification of the polymer. Thus, the conversion increases with increasing the CL concentration in the reaction medium. The degree of polymerization increases with increasing CL concentration passing through a maximum value (corresponding to about 3.3 mol CL/l). The decrease of the polymerization degree for higher monomer concentration values is related to the characteristics of the reaction medium, these being close to those corresponding to bulk polymerization. As a consequence, the high amount of catalyst used in this investigation induces a considerable decrease in the degree of polymerization.

Due to some factors, such as the reduced degree of dissociation of lactam salt, polar impurities from solvent, lower concentration of CL, etc., the anionic polymerization performed in solvents requires large amounts of catalyst. The conversion increases significantly with the increasing of the catalyst amount up to about 5.4 mol % RedAl/mol CL. Subsequently, increasing the catalyst amount determines only a slight increase of the conversion. On

Table I Reaction Conditions and Some Characteristics of Anionic Polycaproamide Obtained in Ethylbenzene

	Reaction Conditions					
Sample No.	Temperature (°C)	[CL] (mol/L)	[RedAl] [(mol %)/(mol CL)]	[IDI]/[RedAl] [(equiv NCO)/mol]	Yield[a] (%)	P_η[b]
1.	80[c]	3.0	3.5	1.0	16.5	78
2.	90[c]	3.0	3.5	1.0	30	113
3.	105[c]	3.0	3.5	1.0	50.4	176
4.	120	3.0	3.5	1.0	67	212
5.	130	3.0	3.5	1.0	70.5	225
6.	140	3.0	3.5	1.0	72	237
7.	130	1.75	3.5	1.0	26	137
8.	130	2.25	3.5	1.0	62.5	203
9.	130	4.55	3.5	1.0	79.5	190
10.	130	3.0	1.98	1.0	45	210
11.	130	3.0	5.4	1.0	78.8	189
12.	130	3.0	6.6	1.0	81.4	153
13.	130	3.0	3.5	0.25	48	195
14.	130	3.0	3.5	0.5	67.7	268
15.	130	3.0	3.5	0.67	73.5	287
16.	130	3.0	3.5	2.0	64	146

Polymerization time, 20 min, except as noted.
[a] Calculated from the conversion of CL to polymer.
[b] Viscometric average polymerization degree.
[c] Polymerization time, 60 min.

the other hand, the degree of polymerization initially increases passing through a maximum value at about 3.5 mol % RedAl/mol CL; for higher catalyst concentrations, the polymerization degrees strongly decrease.

In contrast to the bulk polymerization (characterized by an optimal activator/catalyst = 1 ratio),[22] due to the lower degree of dissociation of the caprolactam salt in nonpolar media, the optimal activator/catalyst ratio we determined was < 1. Within the studied limits of the activator/catalyst ratios, both conversion and the degree of polymerization pass through a maximum, whose position corresponds to a ratio of about 0.67 equiv NCO/mol Red Al.

It thus appears that the most adequate reaction conditions we found were the following: temperatures above 120°C, concentrations of CL in the range of 2.6–3.8 mol CL/L, catalyst concentrations in the range of 2.8–3.6 mol % RedAl/mol CL, and an activator/catalyst ratio in the 0.6–0.7 equiv —NCO/mol RedAl range.

Morphology

The external surface of the granules was investigated using scanning electron microscopy. The synthetized granules have the diameter predominantly in a range of 250–500 μm and a small fraction (below 5% by weight) is outside this range. Highly asymmetric and irregularly shaped particles are obtained as illustrated in Figure 1(a). As shown more clearly in Figure 1(b), these represent, in fact, agglomerates of a great number of small particles. Some granules depict voids in their structure, as shown in Figure 1(b), their external surface being also highly irregular. In addition, the external surface of the individual particles composing the granules is also irregular. As shown in Figure 1(c–f), the external surface of the particles exhibit a great number of needlelike and globular formations. The needlelike formations from Figure 1(c,d) are crystals of pure, unremoved caprolactam.

Through mechanical dispersion of the granules, the particles can be easily individualized [Fig. 2(a)]. As shown in Figure 2(b,c), following the mechanical milling their surface becomes smoother, the above mentioned needlelike and globular formations being removed.

The particles are hard and dense, characterized by a low porosity, and a very small number were broken by mechanical milling. The majority are spherical, with diameters in a range of 2–20 μm, and

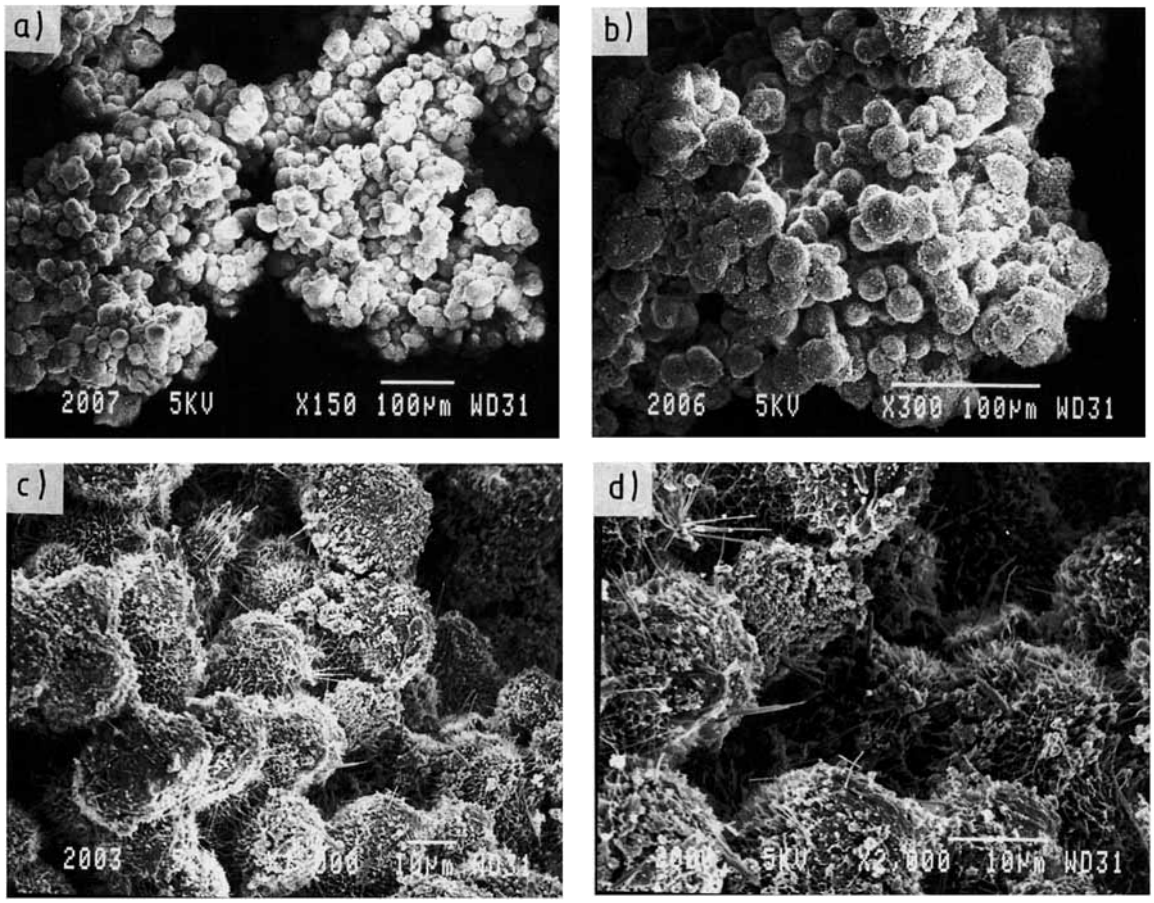

Figure 1 SEM of granular powders (sample no. 5 in Table I): (a, b) low magnification showing the irregular shape of granules (note the voids in the structure); (c, d) medium magnification showing the rough external surface of the particles (note the globular formations and the pure caprolactam crystals); (e, f) high magnification showing the details of particles' surface.

a relatively small number reach up to 40 μm in diameter or have irregular shapes.

Particle size distribution was evaluated through a mathematical processing of the data yielded by direct measurements on photomicrographs. Function of their diameters, all particles were divided into 11 dimensional classes.

The class interval was determined according to the following relation:

$$i = \tfrac{1}{100} \times 8 \times (D_{max} - D_{min}) \quad (1)$$

where D_{max} is the diameter of the greatest measured particle (D_{max} = 44 μm); D_{min} is the diameter of the smallest measured particle (D_{min} = 1 μm). Solving eq. (1), one obtains the value of i = 3.44 μm, and the value i = 4 μm was adopted for further calculations. The histogram from Figure 3 shows the frequency of diameters in each interval. It is evident that the diameters are grouped around the interval from 4 to 16 μm and that there are relatively few very bulky particles.

The average diameter was calculated by statistical processing of these data.[23] As arbitrary average diameter the value of D_0 = 13.5 μm was used, and subsequently the average diameter was calculated from the relation:

$$\bar{D} = D_0 + \frac{\sum n_i \cdot D_i'}{N} \times \frac{1}{l} \quad (2)$$

where n_i is the number of particles of a dimensional class, i; $D_i' = l(D_i - D_0)$, where l can be 10, 100, etc., depending on the number of decimals with which the data are considered; N is the number of measured particles (N = 207).

Dispersion of selection was calculated from the following relationship:

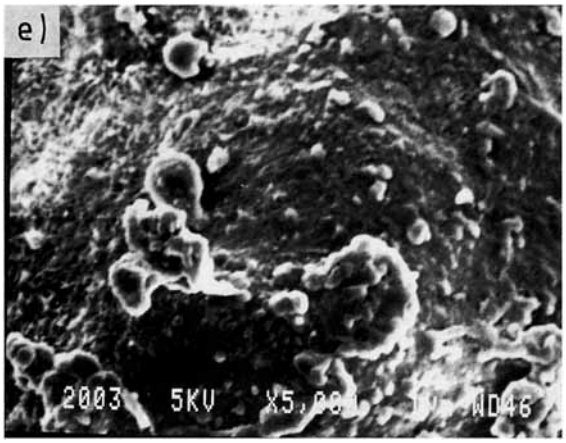

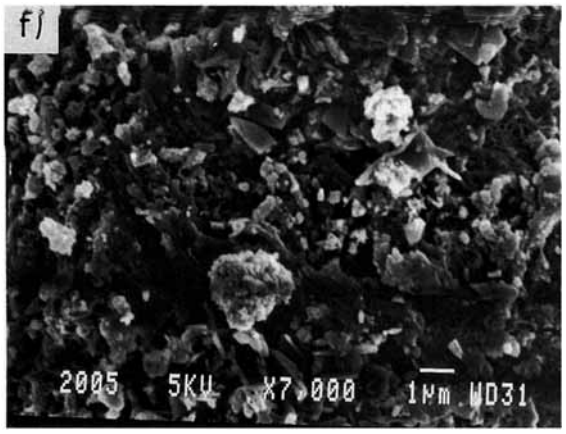

Figure 1 (*Continued from the previous page*)

$$s^2 = \frac{\left|\sum n_i \cdot (D_i')^2 - \frac{(\sum n_i \cdot D_i')^2}{N}\right| \times \frac{1}{l^2}}{N - 1} \qquad (3)$$

The data and the steps involved in the calculation of average diameter are shown in Table II. Using eqs. (2) (3), the values of $\bar{D}$ = 12.57 μm for the average diameter, s^2 = 65.98 for dispersion of selection, and s = 8.12 for the standard deviation were obtained.

To estimate the number of particles composing the granules, we have assumed the following simplifying hypothesis: all particles and granules are spherical, the diameter of all particles is equal to the above calculated average diameter ($\bar{D}$ = 12.57 μm), and the particles are systematically arranged. The systematic arrangement of spheres within a given volume is possible in 10 distinct ways. Corresponding to these, there are four distinct values of the porosities, namely: 0.476, 0.3954, 0.3019, and 0.2595 for the cubic, orthorombic, tetragonal sphenoidal, and rombohedral systems, respectively.[24] The number of particles that compose a granule with a given diameter was calculated using the following relation:

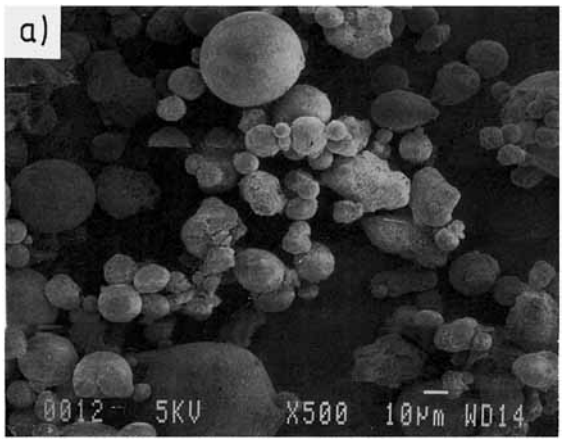

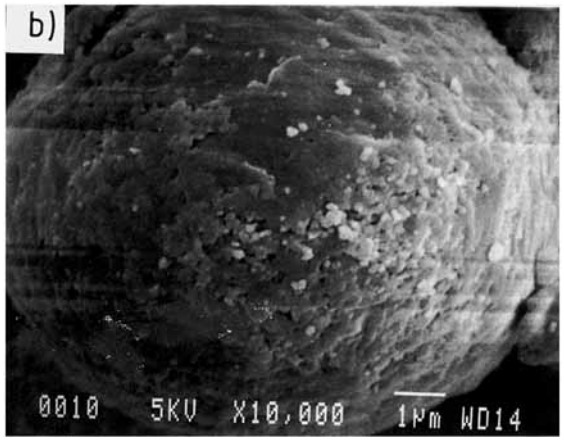

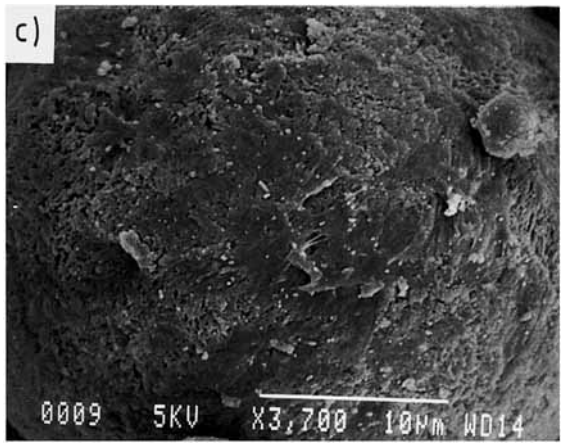

Figure 2 SEM of individualized particles obtained through mechanical milling of granules: (a) low magnification; (b) high magnification showing the external surface of one particle; (c) high magnification showing the external surface of a large particle (note the dense structure).

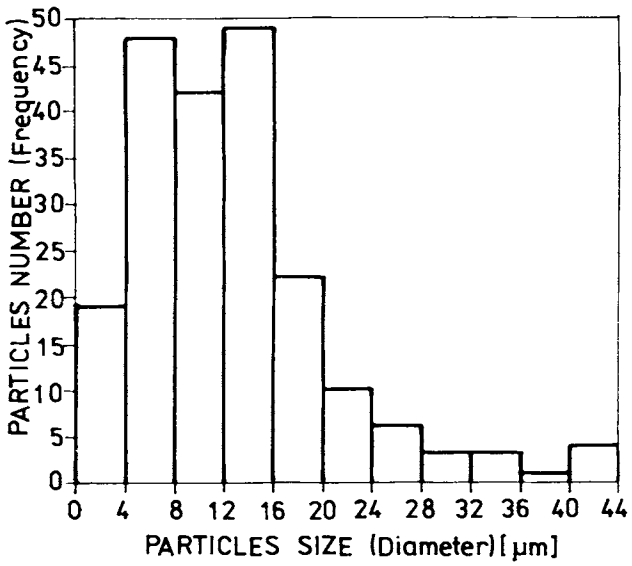

Figure 3 Size distribution of particles which compose the granular powders.

$$n = (1 - p) \times \frac{D_g^3}{\bar{D}^3} \tag{4}$$

where p represents the porosity corresponding to different arrangements of stacked particles, D_g is the diameter of the granules, and $\bar{D}$ is the average diameter of particles ($\bar{D}$ = 12.57 μm). The calculation results for granules having diameters in a range of 250–500 μm are summarized in Table III. It is evident from Table III that the number of particles which compose a granule with a given diameter is very important, thousands or tenfold thousands.

This number strongly increases with increasing the diameter of the granules. However, taking into account both the simplifying hypothesis and the observed voids of the granules it can be assumed that the real number of particles is closer to that calculated, considering high porosity values.

Differential Scanning Calorimetry

The thermal behavior of polycaproamide granules was measured by DSC (Fig. 4). At heating, the melting temperature starts at 195.04°C, giving an endothermic peak with the enthalpy ΔH = 70.07 J/g at 205.33°C. Thus, the anionic polycaproamide obtained in solvent is a semicrystalline polymer. The degree of crystallinity can be calculated from eq. (5).

$$X_c = \frac{\Delta H_i}{\Delta H_f} \times 100\ (\%) \tag{5}$$

where X_c is the degree of crystallinity; ΔH_i is the heat capacity of the investigated sample, i; and ΔH_f is the heat of fusion for 100% crystalline polycaproamide, i.e., 189 J/g.[25,26] The calculated value X_c = 37.4% is slightly lower than that corresponding to the anionic bulk polycaproamide. This behavior is related to the strong undercooling which hinders the development of crystalline structures. At cooling, crystallization starts at 177.66°C, giving an exothermic peak with the enthalpy ΔH = 47.04 J/g.

Table II Data and Steps Involved in the Calculation of Average Diameter of the Particles that Form the Polyamidic Grains

Classes Boundary [μm]	Classes Middle [μm]	n_i	$D_i = \frac{D_i - 13.5}{4}$	$(D_i')^2$	$n_i D_i'$	$n_i(D_i')^2$
0.1–4	2	19	−3	9	−57	171
4.1–8	6	48	−2	4	−96	192
8.1–12	10	42	−1	1	−42	42
12.1–16	14	49	0	0	0	0
16.1–20	18	22	1	1	22	22
20.1–24	22	10	2	4	20	40
24.1–28	26	6	3	9	18	54
28.1–32	30	3	4	16	12	48
32.1–36	34	3	5	25	15	75
36.1–40	38	1	6	36	6	36
40.1–44	42	4	7	49	28	196
				Sums		
		N = 207			$\Sigma n_i D_i'$ = −74	$\Sigma n_i(D_i')^2$ = 876

Table III Correlation between Grain Diameters and the Number of Spherical and Systematically Arranged Particles Composing Them

	Systematic Arrangement of Spheres and Their Porosities			
Grain Diameter [μm]	Cubic (0.476)	Orthorombic (0.3954)	Tetragonal Sphenoidal (0.3019)	Rhombohedral (0.2595)
250	4,132	4,756	5,492	5,825
300	7,123	8,219	9,490	10,066
350	11,311	13,052	15,070	15,985
400	16,885	19,482	22,495	23,862
450	24,041	27,739	32,029	33,975
500	32,979	38,051	43,936	46,605

Sphere diameter is 12.57 μm.

Wide Angle X-Ray Diffraction

Figure 5 shows a representative X-ray diffraction curve of granular polycaproamide. The presence of solvent seems to have no effect on the crystallization form. The prepared polymer contains almost entirely the α-phase. The peak from the crystallographic plane $\alpha_2 = 24°$ (002, 202) (Miller indices are given in parentheses) is more intense than the peak from crystallographic plane $\alpha_1 = 20.3°$ (200). However, a small fraction of polymer crystallized in γ phase: $\gamma_1 = 21.6°$ (002).

On the Formation of Granular Polycaproamide: A Possible Model

To propose an adequate model on the steps involved in the obtaining of granular polycaproamide, it is necessary to take into account both the events occuring in the anionic bulk polymerization (more investigated) and the specific features owing to the presence of solvent in the reaction medium. In the bulk polymerization, the process starts in a homogeneous medium; after a short period of time the viscosity increases strongly, due to polymer formation. As the polymerization proceeds, the polymer solidifies, the temperature being below the melting temperature of the polymer. This step is followed by polymer crystallization. The INTRODUCTION underlined the most important features of the anionic polymerization of CL in the presence of a solvent.

As shown in Figure 6, the polymerization starts in a homogeneous liquid phase (step I in Fig. 6). Chain growth starts in a relatively polar medium. The duration of this step is strongly related to the reaction temperature and to the efficiency of the catalytic system. It decreases with increasing both

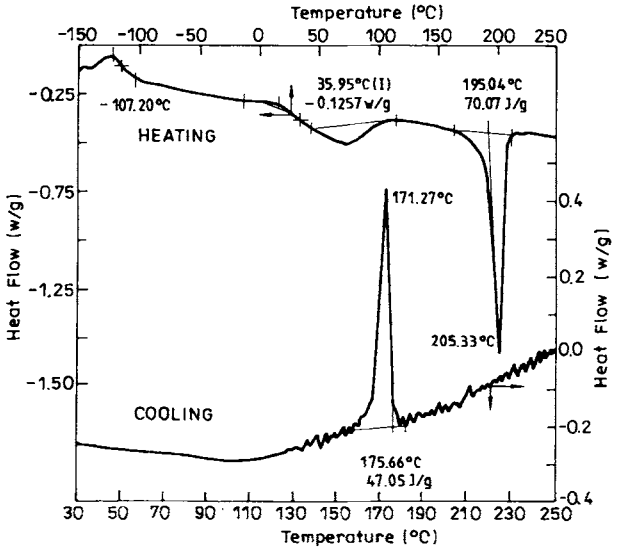

Figure 4 DSC diagram for granular polycaproamide during heating and cooling.

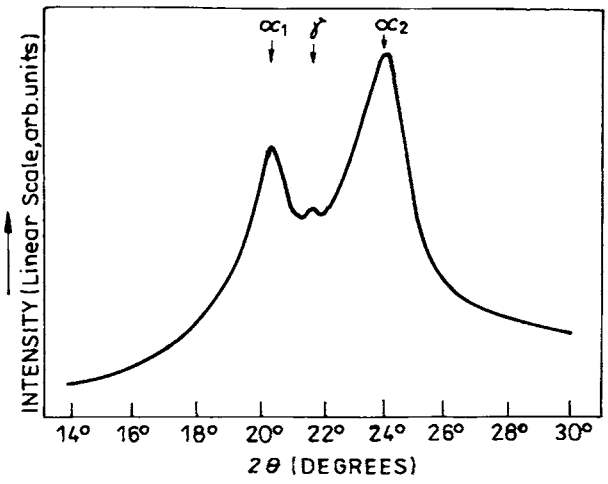

Figure 5 Typical X-ray diffraction curve for granular polycaproamide.

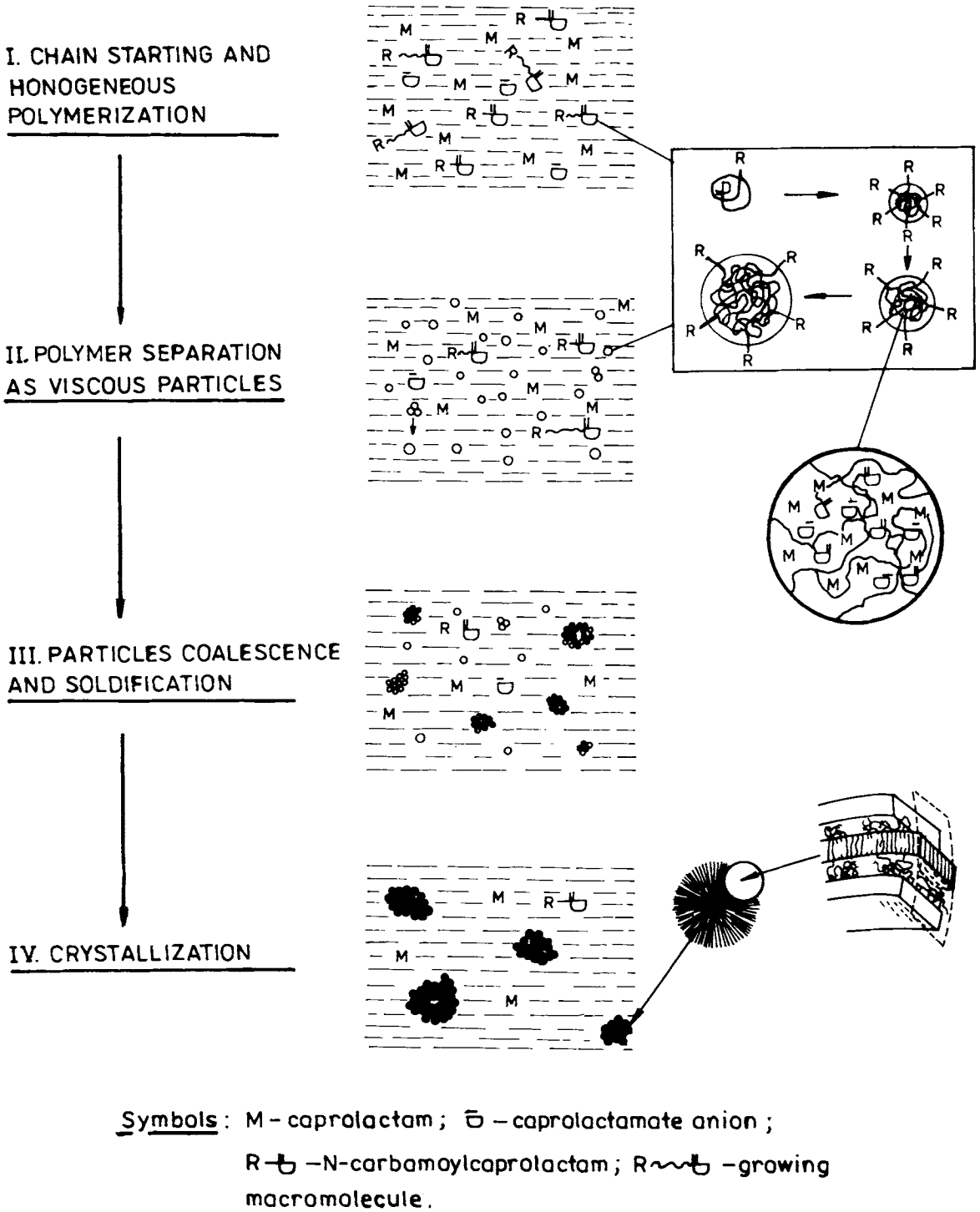

Figure 6 Schematic illustration of stages involved in the obtaining of granular polycaproamide.

the temperature and the efficiency of the catalytic system.

Apart from other activators, in which *N*-acylcaprolactam growing centers are formed stepwise in the reaction medium (e.g., CO_2, esters, carbodiimides, *N*,*N*-disubstituted ureas), by using preformed *N*-acylcaprolactams or acylating reagents that react very quickly with CL (e.g., acid chlorides or isocyanates) the polymerization seems to occur as a particular case of dispersion polymerization.

(Dispersion polymerization may be defined as the polymerization of a monomer dissolved in an organic liquid to produce an insoluble polymer in the form of colloidal dispersion. In a classic process, the colloidal stability of the resulting particles is provided by the absorbtion of an amphiphilic stabilizer or a dispersant that is present in the organic medium on the surface of the polymer particles.)[27]

In the case of the anionic polymerization of CL in solvents, if the polymerization in homogeneous medium proceeds, changes in medium composition decreases the solubility of the growing macromolecules. This favors a quicker precipitation of polymer to form nuclei. These primary particles may undergo aggregation to form colloidal particles (small droplets). Though in this process the stabilizers or the dispersants are not present in the organic medium, one can assume that precipitated macromolecules are oriented with the activator hydrofobic alkyl residues toward the organic nonpolar medium and with the *N*-acyllactam growing centers toward the inside of the (more polar) particles. Thus the external nonpolar groups could determine, to a certain extent, the stability of these primary particles. However, a small fraction of initially separated droplets can then collide and coalesce to form larger droplets, as shown in Figure 2(a). The monomer and the reduced lactam salt are absorbed from the solution by the dispersed polymer phase once it forms, and subsequently almost all of the polymerization process takes place within the monomer-swollen particles (step II in Fig. 6). In this way the nature of particle growth is essentially a microbulk process. Progressive polymerization inside droplets leads to an increase in viscosity, and the dimension of particles increases with the increasing of conversion. This step is also confirmed by the appearance of the "sudden freezing" of the external surface of the particles obtained by mechanical dispersion of granules [Fig. 2(b,c)].

Subsequently, two phenomena occur practically simultaneously: on further collision droplets adhere to one another in the form of fused agglomerates (due to the increasing of both viscosity and particle dimensions when the hydrophobic residues are not able to assure the stability of the particles); and they solidify (due to the important undercooling, i.e., about 70°C below the melting point of the polymer) (step III in Fig. 6). Polymerization can also occur mainly on the external surface of the particles. The globular formations could appear in this stage by addition of the monomer and the catalyst from solvent to the growing centers located close to the external surface.

Finally, the solidified polymer crystallizes (step IV in Fig. 6), and the structure of the granules is established.

In terms of phase separation, in the investigated process, the following phenomena take place: liquid–liquid (L → L) phase, liquid–crystal (L → C) formation, and crystallization,[28] respectively. Because the events from step II to step IV occur in a very short period of time, one could accept that phase and crystal morphology appear in combination. In these circumstances, the phase morphology arises first, within which subsequent crystallization then creates the crystal morphology.

CONCLUSIONS

The anionic polymerization of CL in EB as solvent initiated with $NaH_2[O(CH_2)_2OCH_3]_2Al$ and activated with IDI was studied. Conversions in the range of 16–82% and degrees of polymerization in the range of 78–280 were obtained. The following optimum reaction conditions were determined: temperatures up to 120°C, initial CL concentration of 2.6–3.8 mol/L, catalyst concentration in the range of 2.8–3.6 mol % RedAl/mol CL, and an activator/catalyst ratio in a range of 0.6–0.7 equiv NCO/mol RedAl.

The polymer results as granules having diameters in the range of 250–500 μm. These represent a conglomerate of particles having diameters in a range of 2–40 μm, and were formed through the aggregation of particles during the solidification of the polymer. The most important steps in granule formation are: the growth of the macromolecules in the homogeneous medium, the precipitation and the aggregation to form viscous droplets, progressive polymerization inside the droplets, their aggregation and solidification, and finally the crystallization of polymer. All the above-mentioned processes occur rapidly and partly overlap. The nature of particle growth is related to the nature of the catalytic system. For the investigated system, almost all polymerizations took place within the monomer-swollen particles. The hydrophobic residues of the activator may increase the stability of the particles for a short period of time, after polymer separation.

The polycaproamide obtained by such an approach is a semicrystalline polymer. It contains almost entirely the α-phase.

We wish to express our sincere thanks to Prof. Gerard Riess of the Ecole Nationale Superieure de Chimie de Mulhouse, who kindly supplied us the isophorone diisocyanate and RedAl. We are also grateful to Dr. Frederic Mertz for his assistance in performing the scanning electron microscopy micrographs.

REFERENCES

1. S. Chrzczonowicz, *Zesz. nauk. Politech. Lodz.*, **5,** 65 (1957).
2. S. Chrzczonowicz, M. Wlodarczyk, and B. Ostaszewski, *Makromol. Chem.*, **38,** 159 (1960).
3. W. A. Sahler, Br. Patent, 1.118.700, 1968; *Chem. Abstr.*, **69,** 44630 (1968).
4. U. Keizo, T. Yusaku, and O. Fumimaro, Jap. Patent 68 08833, 1968; *Chem. Abstr.*, **69,** 36596 (1968).
5. M. Biensam and P. Braund, German Patent 1.964.533, 1970; *Chem. Abstr.*, **73,** 67332 (1970); German Patent 1.964.995, 1970; *Chem. Abstr.*, **73,** 78175 (1970).
6. W. P. Wolfers, P. J. Fransen, and J. M. Warnier, *Neth. Appl.*, **70,** 17.791 (1972); *Chem. Abstr.*, **77,** 115108 (1972).
7. W. Kubanek, J. Kralicek, and A. Moucha, *Scientific Paper of the Prague Institute of Chemical Technology,* **C24,** 9 (1976).
8. P. Biernacki and M. Wlodarczyk, *Eur. Polym. J.*, **7,** 739 (1971).
9. P. Biernacki and M. Wlodarczyk, *Eur. Polym. J.*, **11,** 107 (1975).
10. G. Odian, *Principles of Polymerization,* 3rd Ed., John Wiley & Sons, Inc., New York, 1991, p. 562.
11. J. Stehlicek and J. Sebenda, *Eur. Polym. J.*, **22,** 769 (1986).
12. J. Sebenda, in *Comprehensive Chemical Kinetics. Non-Radical Polymerization,* Vol. 15, C. H. Bamford and C. F. H. Tippers, Eds., Elsevier, Amsterdam, 1976, p. 379.
13. C. W. Macosko, *RIM: Fundamentals of Reaction Injection Molding,* Hanser Publishers, Munich, Vienna, New York, 1989, p. 182.
14. P. Biernacki and M. Wlodarczyk, *Eur. Polym. J.*, **16,** 843 (1980).
15. *Polymer Handbook,* 2nd Ed., J. Brandrup and E. H. Immergut, Eds., John Wiley & Sons, Inc., New York 1975, p. IV-27.
16. M. K. Akkapeddi, G. J. Dege, T. D. Gallagher, and M. S. Walsh, in *Recent Advances in Anionic Polymerization,* T. E. Hogen-Esch and J. Said, Eds., Elsevier Science Publishing Co., Inc., 1987.
17. R. Puffr, J. Stehlicek, and J. Sebenda, *Makromol. Chem., Macromol. Symp.*, **60,** 219 (1992).
18. J. Stehlicek, J. Labosky, and J. Sebenda, *Collect. Czech. Chem. Commun.*, **32,** 544 (1967).
19. J. Stehlicek, K. Gehrke, and J. Sebenda, *Collect. Czech. Chem. Commun.*, **32,** 370 (1967).
20. T. M. Frunze, V. A. Kotel'nikov, V. V. Kurashev, Yu. A. Avakyan, L. B. Danilevskaya, and S. P. Davtyan, *Abstracts IUPAC Macro '83, Sec. I, Polym. Chem.*, Bucharest, 1983, p. 233.
21. C. A. Veith and R. E. Cohen, *ACS Polym. Preprints,* **31,** 42 (1989).
22. W. L. Chang, K. C. Frisch, and K. Ashida, *J. Polym. Sci., Polym. Chem. Ed.*, **27,** 3637 (1989).
23. D. Ceausescu, *Utilizarea statisticii matematice in chimia analitica,* Ed. Technica, Bucuresti, 1982, p. 90.
24. *Unit. Operations,* G. G. Brown, D. Kaltz, A. S. Foust, and R. Scheidewind, Eds., Wiley, New York, 1935, p. 215.
25. F. N. Liberti and B. Wunderlik, *J. Polym. Sci.*, **A-36,** 833 (1968).
26. H. H. Wand and M. F. Lin, *J. Appl. Polym. Sci.*, **43,** 259 (1991).
27. Q. Wang, S. Fu, and T. Yu, *Prog. Polym. Sci.*, **19,** 703 (1994).
28. A. Keller, *Macromol. Symp.*, **98,** 1 (1995).

Received February 21, 1996
Accepted April 15, 1996